Applied Mathematics and Mechanics
(English Edition, Vol 25, No 8, Aug 2004)

Published by Shanghai University,
Shanghai, China

 Article ID: 0253-4827(2004)08-0945-06

NUMERICAL SIMULATION OF TRANSIENT THERMAL FIELD IN LASER MELTING PROCESS*

YAO Guo-feng (姚国凤)[1], CHEN Guang-nan (陈光南)[2]

(1. Department of Mechanics, Institute of Mechanical Science and Engineering, Jilin University, Changchun 130025, P. R. China;
2. Institute of Mechanics, Chinese Academy of Sciences, Beijing 100080, P. R. China)

(Communicated by LI Jia-chun)

Abstract: Numerical simulation of thermal field was studied in laser processing. The 3-D finite element model of transient thermal calculation is given by thermal conductive equation. The effects of phase transformation latent are considered. Numerical example is given to verify the model. Finally the real example of transient thermal field is given.

Key words: laser melting process; thermal field; numerical simulation

Chinese Library Classification: TG174 Document code: A

2000 Mathematics Subject Classification: 80A17; 80A22; 80M10

Introduction

With the request of the high-powered surface, surface hardening and modifying have been one of important subjects in the world. Laser melting process is one of the methods of surface hardening and toughening of materials. It is the quick heating and cooling process. It is perfectly different from the common heat treatment, but some problems need solving in laser surface processing, for example, micro-crack on the surface, the one of its main cause is residual stress. In order to deal with the problem, the material micro-structure and residual stress field should be studied with temperature change. Now J. B. Leblond[1], S. Denis[2] group in France and some researchers in our country have been studied the subject.

Numerical simulation of thermal field and residual stress field in laser processing are studied. The 3-D finite element model of transient thermal and residual stress calculation is given. It considers the effects of phase transformation latent[3,4], also thermal, structure and plastic deformation. Finally numerical example is given to verify the model. This is good contribution to

* Received date: 2002-08-15; Revised date: 2004-01-06

Foundation items: the National Natural Science Foundation (Key Project) of China (59836220); the National High Technology Research and Development Program of China (863 Program) (2002AA331180); the National Key Grant Program of Basic (2002CCA01200)

Biography: YAO Guo-feng (1962～), Professor, Doctor (Tel: +86-431-5690930; Fax: +86-431-5705288; E-mail: yaogf@jlu.edu.cn)

study the technology of laser surface processing further.

1 The Finite Element Model

The progress of laser melting surface process is as follows: when laser moves on the work piece, the materials of processed plane begin to heat, generate phase transformation of solid, and then melt with the rise of temperature; after scanning, the materials begin to cool, condense, generate phase change of solid, and finally drops to room temperature, so that the temperature changes of the work piece depend on the heat input model, heat conduction, latent heat of phase transformation and surface heat loss.

By heat conduction equation and its boundary conditions, the variational formulation is obtained, and then applying variational rule and assuming the temperature is obtained at time t, the thermal equilibrium equation corresponding to time $t + \Delta t$ is given by[3,5]

$$\int_V \delta T^{\mathrm{T}}\, {}^{t+\Delta t}K\, {}^{t+\Delta t}T\, \mathrm{d}V = {}^{t+\Delta t}Q + \int_c \delta T^{\mathrm{s}}\, {}^{t+\Delta t}h({}^{t+\Delta t}T_{\mathrm{e}} - {}^{t+\Delta t}T^{\mathrm{s}})\, \mathrm{d}s + \int_r \delta T^{\mathrm{s}}\, {}^{t+\Delta t}\kappa_{\mathrm{r}}({}^{t+\Delta t}T_{\mathrm{e}} - {}^{t+\Delta t}T^{\mathrm{s}})\, \mathrm{d}s, \tag{1}$$

where

$${}^{t+\Delta t}Q = \int_s \delta T\, {}^{t+\Delta t}q^{\mathrm{s}}\, \mathrm{d}s + \int_V \delta T({}^{t+\Delta t}\tilde{q}^{\mathrm{B}} - {}^{t+\Delta t}(\rho c)\, {}^{t+\Delta t}\dot{T})\, \mathrm{d}V. \tag{2}$$

In Eqs. (1) and (2), T is the temperature variable; T^{s} is the surface temperature variable; T_{e} is the ambient temperature; h is the surface convective heat transfer coefficient, $\kappa_{\mathrm{r}} = \sigma\varepsilon(T_{\mathrm{e}}^2 + (T^{\mathrm{s}})^2)(T_{\mathrm{e}} + T^{\mathrm{s}})$ is the surface radiation heat transfer coefficient; σ is the Stefan-Boltzmann constant, ε is the emissivity; T' is the temperature gradient; K is the matrix of heat conduction coefficient; q^{s} is the surfce heat flow input density; q^{B} is the internal heat generation density; ρ is the mass density; c is the specific heat coefficient.

Linearizing Eq. (1) and applying Newton-Raphson iteration method as well as implicit time integration, the iterative formulation of temperature increment is obtained. Employing the 8-node block element discretization, the finite element equation of temperature increments is obtained by[6,7]

$$({}^{t}K^{\mathrm{k}} + {}^{t}K^{\mathrm{c}} + {}^{t}K^{\mathrm{r}})\Delta T^{(i)} = {}^{t+\Delta t}Q^{(i)} + {}^{t+\Delta t}Q^{\mathrm{c}(i-1)} + {}^{t+\Delta t}Q^{\mathrm{r}(i-1)} - {}^{t+\Delta t}Q^{\mathrm{k}(i-1)}, \tag{3}$$

where

$$\begin{cases} {}^{t}K^{\mathrm{k}} = \int_V \bar{B}^{\mathrm{T}}\, {}^{t}K\bar{B}\, \mathrm{d}V, \quad {}^{t}K^{\mathrm{c}} = \int_c {}^{t}h H^{\mathrm{sT}} H^{\mathrm{s}} \mathrm{d}s, \quad {}^{t}K^{\mathrm{r}} = \int_r {}^{t}\kappa_{\mathrm{r}} H^{\mathrm{sT}} H^{\mathrm{s}} \mathrm{d}s, \\ {}^{t+\Delta t}Q^{(i)} = {}^{t+\Delta t}\tilde{Q} - {}^{t+\Delta t}C^{(i-1)}\, {}^{t+\Delta t}\dot{T}^{(i)} + {}^{t+\Delta t}Q_{\mathrm{lat}}^{(i-1)}, \\ {}^{t+\Delta t}\tilde{Q} = \int_s H^{\mathrm{sT}}\, {}^{t+\Delta t}q^{\mathrm{s}} \mathrm{d}s, \\ {}^{t+\Delta t}C^{(i-1)} = \int_V {}^{t+\Delta t}(\rho c)^{(i-1)} H^{\mathrm{T}} H \mathrm{d}V, \\ {}^{t+\Delta t}Q^{\mathrm{c}(i-1)} = \int_c {}^{t+\Delta t}h^{(i-1)} H^{\mathrm{sT}}[H^{\mathrm{s}}({}^{t+\Delta t}T_{\mathrm{e}} - {}^{t+\Delta t}T^{(i-1)})]\mathrm{d}s, \\ {}^{t+\Delta t}Q^{\mathrm{r}(i-1)} = \int_r {}^{t+\Delta t}\kappa_{\mathrm{r}}^{(i-1)} H^{\mathrm{sT}}[H^{\mathrm{s}}({}^{t+\Delta t}T_{\mathrm{e}} - {}^{t+\Delta t}T^{(i-1)})]\mathrm{d}s, \\ {}^{t+\Delta t}Q^{\mathrm{k}(i-1)} = \int_V \bar{B}^{\mathrm{T}}\, {}^{t+\Delta t}K^{(i-1)}\, \bar{B}\, {}^{t+\Delta t}T^{(i-1)} \mathrm{d}V. \end{cases} \tag{4}$$

In the above formulations, H is the matrix of shape functions about eight-node solid; $\overline{B}$ is the derivative matrix of shape functions, H and B are as shown in Refs. [6,7].

Letting

$$ {}^{t+\Delta t}\dot{T}^{(i)} = ({}^{t+\Delta t}T^{(i-1)} + \Delta T^{(i)} - {}^{t}T)/\Delta t. \tag{5} $$

Substituting Eq. (5) into Eq. (3),

$$ ({}^{t}K^{k} + {}^{t}K^{c} + {}^{t}K^{r} + {}^{t+\Delta t}C^{(i-1)}/\Delta t)\Delta T^{(i)} = {}^{t+\Delta t}Q^{c(i-1)} + {}^{t+\Delta t}Q^{r(i-1)} - {}^{t+\Delta t}Q^{k(i-1)} + {}^{t+\Delta t}\tilde{Q} - {}^{t+\Delta t}C^{(i-1)}({}^{t+\Delta t}T^{(i-1)} - {}^{t}T)/\Delta t + {}^{t+\Delta t}Q_{lat}^{(i-1)}, \tag{6} $$

where ${}^{t}K^{k}$, ${}^{t}K^{c}$ and ${}^{t}K^{r}$ are conduction, convection and radiation matrix, respectively; ${}^{t+\Delta t}Q_{lat}^{(i-1)}$ is the latent heat vector; ${}^{t+\Delta t}Q^{c(i-1)}$ is the heat loss vector of convection in step $i-1$; ${}^{t+\Delta t}Q^{r(i-1)}$ is the heat loss vector of radiation in step $i-1$; ${}^{t+\Delta t}Q^{k(i-1)}$ is the conductive vector in step $i-1$.

If the temperature distributions of time t and step $i-1$ of time $t+\Delta t$ are calculated, the temperature distributions of step i of time $t+\Delta t$ are obtained by solving Eq. (6)

$$ {}^{t+\Delta t}T^{(i)} = {}^{t+\Delta t}T^{(i-1)} + \Delta T^{(i)}. \tag{7} $$

Computing of latent heat ${}^{t+\Delta t}Q_{lat}^{(i-1)}$ in finite element method:

1) Latent heat of fluid-solid phase change

At node k, when the temperature of the node k is in the interval of fluid-solid phase change, the latent heat increment is

$$ \Delta Q_{l,k}^{(i)} = -\int \frac{1}{\Delta t}\rho c^{*}({}^{t+\Delta t}T_k^{(i)} - T_f)\,dV = \frac{(T_f - {}^{t+\Delta t}T_k^{(i)})}{\Delta t}C^{*}m_k, \tag{8} $$

where m_k is the accumulative mass of node k; T_f is the material melting point; C^{*} is expressed as

$$ C^{*} = 1\Big/\left\{\left(\frac{\Delta T_f}{L}\right) + \left(\frac{1}{{}^{t+\Delta t}C^{(i-1)}}\right)\right\}, \tag{9} $$

where ΔT_f is temperature interval of fluid-solid phase change; L is the latent heat coefficient. Therefore, the latent heat of step i at the node k is given by

$$ {}^{t+\Delta t}Q_{l,k}^{(i)} = {}^{t+\Delta t}Q_{l,k}^{(i-1)} + \Delta Q_{l,k}^{(i)}, \tag{10} $$

when the temperature of node k doesn't reach the interval of phase change, the corresponding latent heat is zero.

2) Latent heat of solid phase change

At node k, when the temperature reaches the phase change temperature of some solid phase, the latent heat increment is computed by

$$ \Delta Q_{l,k}^{(i)} = m_k H^{*}\frac{\Delta F_k}{\Delta t}, \tag{11} $$

where H^{*} is the heat transfer coefficient; ΔF_k is phase change increment of some phase at step i. The fractions of non-martensitic phase are obtained by Avrami equation

$$ F_k = 1 - \exp[-b_k t^{n_k}], \tag{12} $$

where b_k, n_k are constants with the change of temperature, which can be obtained by C-C-T curve and T-T-T curve. The martensitic fraction is calculated through Koistinen-Marburger equation

$$ F_k = 1 - \exp[-0.011(M_s - T_k)], \tag{13} $$

where M_s is the martensitic start temperatue; T_k is the temperature of node k. By Eq. (10), the phase change latent heat of node k can be obtained.

The convergence criterion of iteration is as follows:

$$\frac{\left[\sum_{k=1}^{N}\left\{T_k^{(i)}\right\}^2-\sum_{k=1}^{N}\left\{T_k^{(i-1)}\right\}^2\right]^{1/2}}{\left[\sum_{k=1}^{N}\left\{T_k^{(1)}\right\}^2\right]^{1/2}}\leq R_{\mathrm{tol}}, \tag{14}$$

where N is the number of nodes; R_{tol} is the tolerance error. At each iterative step, after the temperatures of all nodes are calculated, verify the Eq. (14), if it is right, compute next time step; if not, continue to iterate until converge.

Based on the method, the numerical simulation program of the thermal field is completed. Applying the soft, the temperature distributions of work piece are obtained.

2 Verification of the Model

Because the measure of temperature is very difficult in laser melting process, the model of Ref. [8] is adopted to verify the present model. The model of Ref. [8] is the electrical arc welding model, which is different from laser melting process about heat input model, melting and solidifying speed and phase transformation. Except some sub-program, the other computing blocks are the same. The work piece is 8 cm long, 20 cm wide and 10 cm thick low carbon structural stell (0.23 pct C); the welding speed is 5 mm/s; the heat input model[4] is

$$q_{\mathrm{f}}(x,y,z,t)=\frac{6\sqrt{3}f_{\mathrm{f}}Q}{ab_1c\sqrt{\pi}}\mathrm{e}^{-3x^2/a^2}\mathrm{e}^{-3y^2/b_1^2}\mathrm{e}^{-3[z+v(\tau-t)]^2/c^2}, \tag{15}$$

$$q_{\mathrm{r}}(x,y,z,t)=\frac{6\sqrt{3}f_{\mathrm{r}}Q}{ab_2c\sqrt{\pi}}\mathrm{e}^{-3x^2/a^2}\mathrm{e}^{-3y^2/b_2^2}\mathrm{e}^{-3[z+v(\tau-t)]^2/c^2}, \tag{16}$$

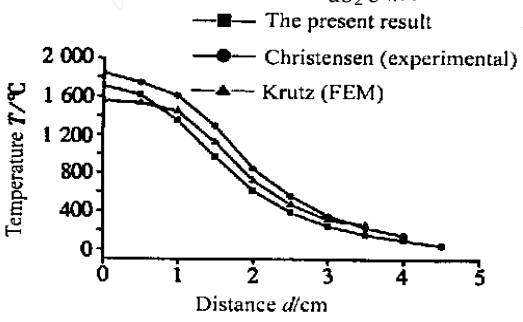

Fig. 1 Some temperature distributions along the top of the work piece perpendicular to the weld

where $q_{\mathrm{f}}(x,y,z,t)$ and $q_{\mathrm{r}}(x,y,z,t)$ are front and rear quadrant heat input density, respectively; $\xi=z+v(\tau-t)$ is the coordinate transformation about the fixed and moving coordinate system; $f_{\mathrm{f}}+f_{\mathrm{r}}=2$; $f_{\mathrm{f}}=0.6$, $f_{\mathrm{r}}=1.4$ in the present model; $a=2.0$ cm, $b_1=1.5$ cm, $b_2=3.0$ cm, $c=2.0$ cm, $Q=36\,568.35$ W. The work piece is divided to 3 968 elements. Applying the model to compute the transient temperature distributions, the temperature distributions along the top of the work piece perpendicular to the weld 11.5 s after the heat source has passed the reference plane is compared with the results of Ref. [8] in Fig. 1.

From Fig. 1, the present model is available.

3 The Temperature Distributions of Laser Melting Process

Apply the present model to calculate the transient thermal field distributions of work peice in laser melting process. The material of work piece is the same as one of Section 2, the work piece is 24 mm long, 20 mm wide and 10 mm thick; laser power $P=1\,000$ W, absorptivity $A=0.70$, transverse speed $v=20$ mm/s and characteristic radius of heat flux distribution $r=2$ mm. By the present model, each point temperature of work piece can be obtained at any time. The

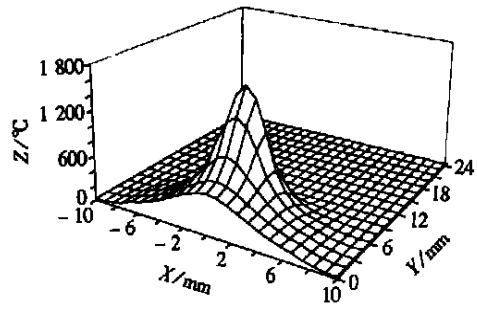

Fig. 2 Temperature distribution on 0.5 mm interface at 0.5 s

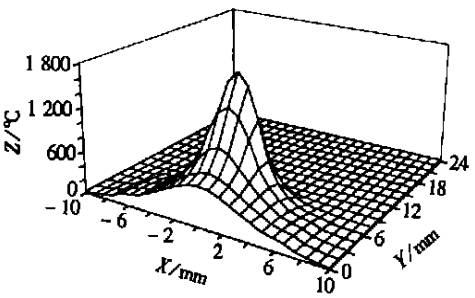

Fig. 3 Temperature distribution on surface at 0.5 s

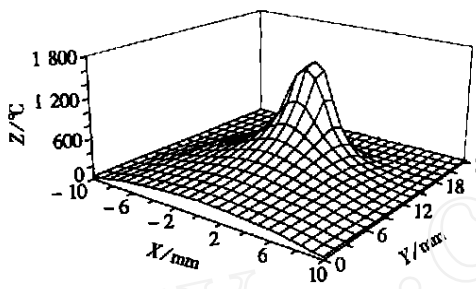

Fig. 4 Temperature distribution on 0.5 mm interface at 1 s

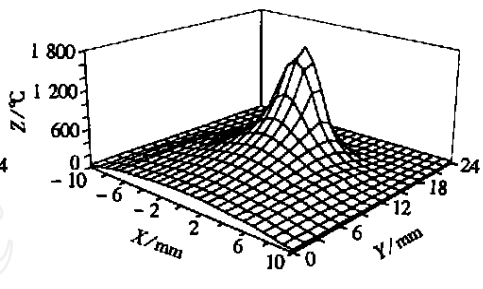

Fig. 5 Temperature distribution on surface at 1 s

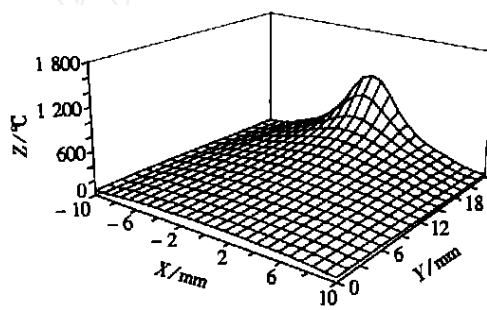

Fig. 6 Temperature distribution on 0.5 mm interface at 1.5 s

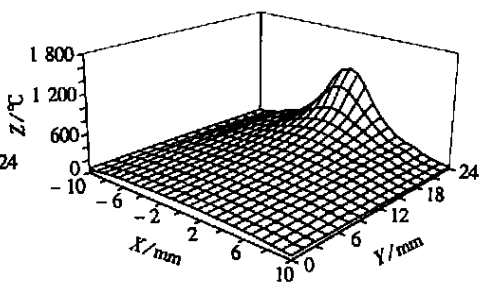

Fig. 7 Temperature distribution on surface at 1.5 s

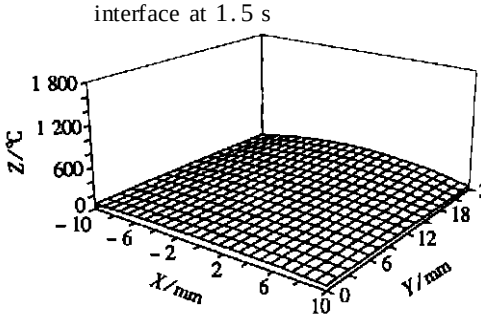

Fig. 8 Temperature distribution on 0.5 mm interface at 2 s

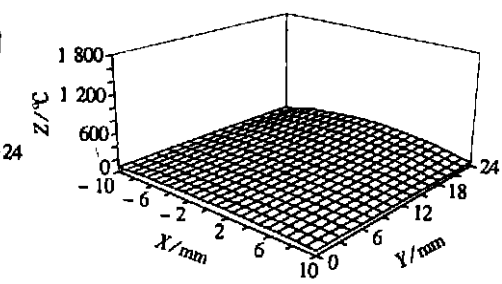

Fig. 9 Temperature distribution on surface at 2 s

section only gives the results of top surface and interface 0.5 mm from the top surface as shown in Figs. 2～9.

4 Results and Discussion

From Fig. 1, the present results are better than the others, but there is also a error compared with the experimental result. The reasons of the error are as follows: 1) The error of the 8-node block element; 2) The error of thermo-physical coefficient; 3) The accumulation of the each step error. The main reasons are 1) and 2). First, the measuring of thermo-physical coefficients is very difficult in high temperature, which can only be obtained by extrapolation of low temperature data, so the erros must exist; secondly, the error of high degree of free (DOF) element is smaller than those of low DOF element, but its computing quantity increases with high speed, it costs the CPU time, so 8-node element is adopted in the reasonable error range. From Figs. 2～9, the results are consistent with qualitative analysis.

Acknowledgements This project was supported by the National High Technology Research and Development Program of China (863 Program) (Grant No. 2002AA331180), the National Key Grant Program of Basic (Grant No. 2002CCA01200), the National Natural Science Foundation (59836220) and the Key Laboratory on Bionic Technique of ground machine (Jilin University). Thanks for the help of the Network Center of the Chinese Academy of Sciences. The authors are grateful to reviewers for their helpful suggestions and discussions.

References:

[1] Leblond J B, Mottet G, Devaux J C. Theoretical and numerical approach to the plastic behaviour of steels during phase transformations — I: Derivation of general relations[J]. Journal of the Mechanics and Physics of Solids, 1986, **34**(4): 395 - 409.

[2] Denis S, Farias D, Simon A. Mathematical model coupling phase transformations and temperature evolutions in steels[J]. ISI J International, 1992, **32**(3): 316 - 325.

[3] Donald Rolph W, Bathe K J. An efficient algorithm for analysis of nonlinear heat transfer with phase changes[J]. International Journal for Numerical Methods in Engineering, 1982, **18**: 119 - 134.

[4] Prakash K, Agarwal, Brimacombe J K. Mathematical model of heat flow and austenite-pearlite transformation in eutectoid carbon steel rods for wire[J]. Metallurgical Transactions B, 1981, **12**: 121 - 133.

[5] Bathe K J, Khoshgoftaar M R. Finite element formulation and solution of nonlinear heat transfer [J]. Nuclear Engineering and Design, 1979, **51**: 389 - 401.

[6] WANG Xu-cheng, SHAO Min. Fundamental Principle and Numerical Method of Finite Element [M]. Beijing: Tsinghua University Press, 1996: 421 - 442. (in Chinese)

[7] MA Dian-ying, WANG Jia-lin. Finite Element Foundation[M]. Jilin: Jilin Science and Technology publishing House, 1990, 109 - 115. (in Chinese)

[8] Goldak J, Chakravarti A, Bibby M. A new finite element model for welding heat sources[J]. Metal Trans, 1984, **15**: 299 - 305.